ACS APPLIED MATERIALS & INTERFACES

www.acsami.org

Research Article

Novel BODIPY-Based Photobase Generators for Photoinduced Polymerization

Shupei Yu, Ojasvita Reddy, Alperen Abaci, Yongling Ai, Yanmei Li, Hao Chen, Murat Guvendiren, Kevin D. Belfield,* and Yuanwei Zhang*

Cite This: *ACS Appl. Mater. Interfaces* 2023, 15, 45281−45289

Read Online

ACCESS | Metrics & More | Article Recommendations | Supporting Information

ABSTRACT: Photobase generators (PBGs) are compounds that utilize light-sensitive chemical-protecting groups to offer spatio-temporal control of releasing organic bases upon targeted light irradiation. PBGs can be implemented as an external control to initiate anionic polymerizations such as thiol−ene Michael addition reactions. However, there are limitations for common PBGs, including a short absorption wavelength and weak base release that lead to poor efficiency in photopolymerization. Therefore, there is a great need for visible-light-triggered PBGs that are capable of releasing strong bases efficiently. Here, we report two novel BODIPY-based visible-light-sensitive PBGs for light-induced activation of the thiol−ene Michael "click" reaction and polymerization. These PBGs were designed by connecting the BODIPY-based light-sensitive protecting group with tetramethylguanidine (TMG), a strong base. Moreover, we exploited the heavy atom effect to increase the efficiency of releasing TMG and the polymerization rate. These BODIPY-based PBGs exhibit extraordinary activity toward thiol−ene Michael addition-based polymerization, and they can be used in surface coating and polymer network formation of different thiol and vinyl monomers.

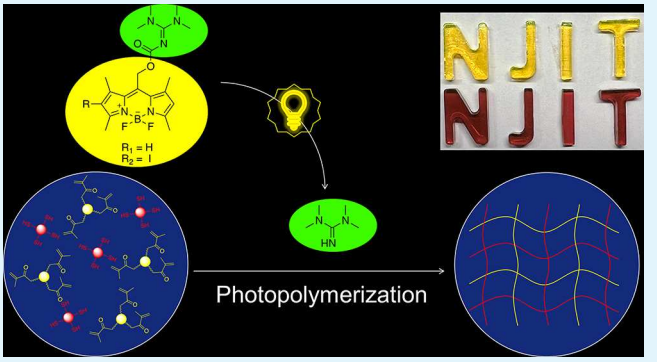

KEYWORDS: *photobase generator, thiol−ene Michael reaction, LED light, BODIPY, photopolymerization*

INTRODUCTION

Since the definition of a "click reaction" by Sharpless and co-workers in 2001,[1] this concept has been employed to great effect in bioconjugation, drug synthesis, materials science, and radiochemistry.[2] Among "click" reactions, the base-catalyzed thiol−ene Michael addition reaction is considered a prized tool in materials synthesis, which provides high functional group conversion, high reaction rate, and mild reaction conditions.[3] The thiol−ene Michael reaction proceeds via an anion-mediated pathway, in which a base deprotonates a thiol, forming a thiolate anion that reacts with electron-deficient alkenes to generate a thioether bond.[4] The versatility of the thiol−ene Michael reaction has been implemented in polymer science, including polymer-based gene delivery systems,[5] dendrimer synthesis,[6,7] polymer surface modification,[8,9] 3D printing,[10−12] hyperbranched polymers,[13,14] and other polymer syntheses.[15] However, it is still challenging to provide the spatial and temporal control for the thiol−ene Michael reaction, because the polymerization reaction is initiated immediately after the introduction of the base.[16] To address this issue, photobase generators (PBGs) have been utilized, which provide photoinduced control and are capable of releasing base species under irradiation of light at a specific wavelength.

PBGs are a series of photosensitive compounds, which absorb the incident light and then release the basic species that can deprotonate a thiol and trigger the consequent reactions. The ideal characteristics of PBGs include (1) strong absorption in the visible region; (2) high quantum yield to generate a base; and (3) chemical stability in the dark before photolysis.[17] Compared with photoacid generators (PAGs), PBGs are much less developed and the common structures are based on quaternary ammonium salts (QAs),[18−20] tetraphenylborate salts (TBD),[21] and carbamates.[22−24] Most of these common PBGs are only able to liberate relatively weak primary and secondary amines that are generally inefficient in the activation of anionic polymerizations.[25] For example, Sarker's group utilized QAs to generate tertiary amines upon UV light irradiation.[18,26] In addition, due to the weak bases released, the system still needs a second thermal treatment to form the polymeric network, which may affect the final polymer

Received: June 28, 2023
Accepted: September 1, 2023
Published: September 14, 2023

Scheme 1. Synthesis of BODIPY-TMG and BODIPY-I-TMG

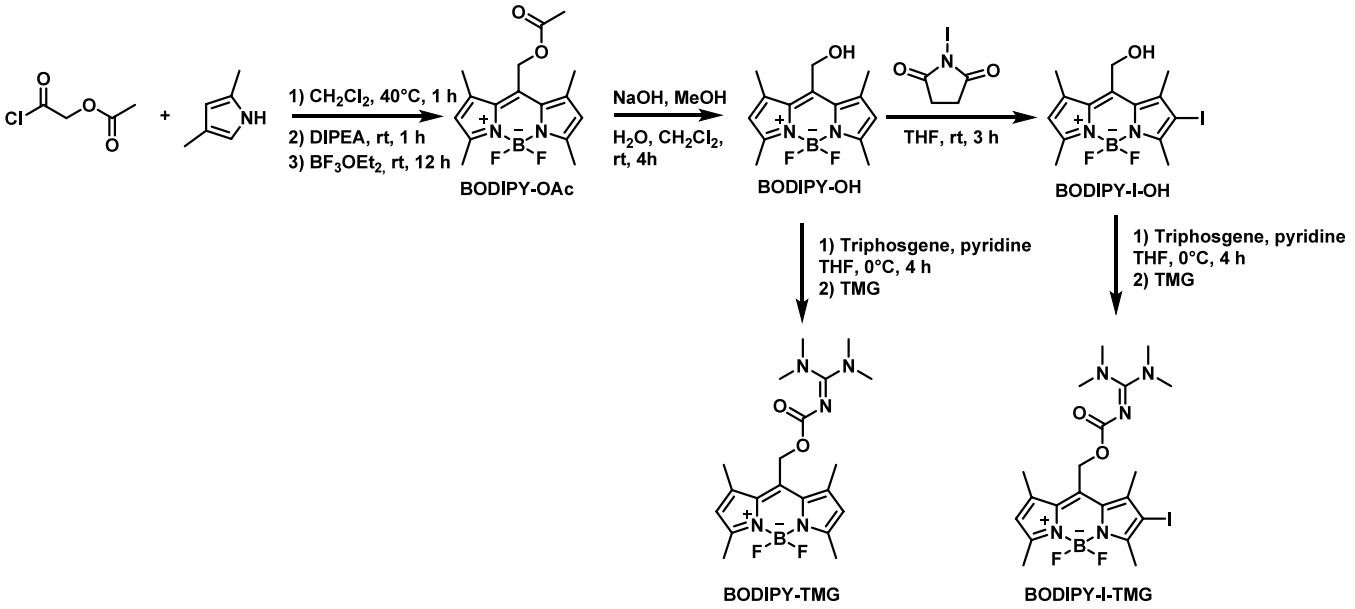

structure. Another challenge that remains in the field is the design and synthesis of visible-light-sensitive PBGs.[25] Most typical PBGs absorb strongly only under high-energy UV and/or blue light, which presents a series of disadvantages including (1) causing irreversible damage to cells and tissues limiting their applications in biological environments and (2) shallow light penetration depth.[27] Recently, there has been increasing interest in the development of photoinitiators that work under visible-light excitation, and the popularity of energy-efficient LED light paved the way for low energy consumption and low heat generation. For example, Hillet et al. reported a photopolymerziation approach for facial soft tissue restoration in small animals[28] and Pioletti et al. studied the photopolymerization process of a hydrogel behind a soft tissue.[29] For these reasons, new classes of photobase systems were reported by Bowman et al., who utilized 2-(2-nitrophenyl)-propyloxycarbonyl (NPPOC), (3,4-methylenedioxy-6-nitrophenyl)-propyloxycarbonyl (MNPPOC), and coumarin as photolabile protecting groups (PPGs) to photocage the strong base 1,1,3,3-tetramethylguanidine (TMG, pK_a = 13.6).[24,30] In another work, Engelke and Truong reported a thioxanthone-based structure for 1,8-diazabicyclo[5.4.0]undec-7-ene (DBU) release under blue light and used this for polymer cross-linking.[31] Although these reports extended the excitation wavelengths, the compounds based on coumarin and thioxanthone are still absorbed primarily in the blue region, around 400 nm. Therefore, there is an urgent need for novel PBGs that can generate strong bases with absorption at wavelengths further in the visible range for deep tissue regeneration and engineering.

Compared with chromophores used in the reported PBGs (such as nitrobenzene or coumarin), BODIPY (boron-dipyrromethene) derivatives have several advantageous properties, such as stability in various media, sharp absorbance spectra, high molar absorptivity, low toxicity, high quantum yields, and color shifts by simple structure modification.[32] For these reasons, BODIPY derivatives have experienced wide use as fluorescent probes,[33−37] photocatalysts,[38,39] photosensitizers in photodynamic therapy,[40,41] and cell visualization agents[42,43] in biolabeling,[44−46] and bioimaging.[47,48] Recently, Winter and co-workers reported a family of BODIPY-derived photocages that can release carboxylic acid under targeted light irradiation. The BODIPY core in the 3,5 meso-position was modified with different substituents to adjust conjugation and hydrophilic properties, which greatly changed the λ_{max} and deprotection efficiency of the target molecule.[49,50] Moreover, Sitkowska and co-workers reported a series of BODIPY-based photoprotecting groups for primary and secondary amines.[32] Inspired by these promising findings, we designed novel BODIPY-based PBGs that utilized the BODIPY core as the photocage and TMG as the leaving group, while retaining the excellent photophysical properties of BODIPYs. The strong basicity of TMG is used to efficiently trigger the thiol−ene Michael addition reactions in a light-guided manner. Moreover, to improve the photouncaging efficiency, heavy-atom iodine was introduced to the BODIPY structure (BD-I-TMG).[51] Compared with the derivative without iodine (BD-TMG), BD-I-TMG exhibited increased intersystem crossing (ISC) and, consequently, improved the release of TMG from the long-lived triplet excited state.[52]

To investigate the photoactivating abilities of BD-TMG and BD-I-TMG, we employed various thiols and vinyl-containing compounds as model reactions. The reaction kinetics and yields were monitored by ^{1}H NMR. Furthermore, butyl 3-mercaptopropionate and ethyl acrylate were implemented to investigate the photoactivator's efficiency by monitoring the conversion of thiol function groups through FTIR spectral analyses. The synthetic route for BD-TMG and BD-I-TMG is presented in Scheme 1. BD−OH and BD-I−OH were synthesized through a modified version of the reported methods.[32,52] All reactions were conducted under mild conditions.

EXPERIMENTAL SECTION

Materials and Instruments. 2,4-Dimethylpyrrole, *N*,*N*-diisopropylethylamine, and pentaerythritol tetrakis(mercaptoacetate) were purchased from TCI America. Acetoxyacetyl chloride and boron trifluoride diethyl etherate were purchased from Thermo Scientific. Triphosgene, *N*-iodosuccinimide, 1,1,3,3-tetramethylguanidine, butyl thioglycolate, divinyl sulfone, ethyl acrylate, butyl 3-mercaptopropi-

https://doi.org/10.1021/acsami.3c09326
ACS Appl. Mater. Interfaces 2023, 15, 45281−45289

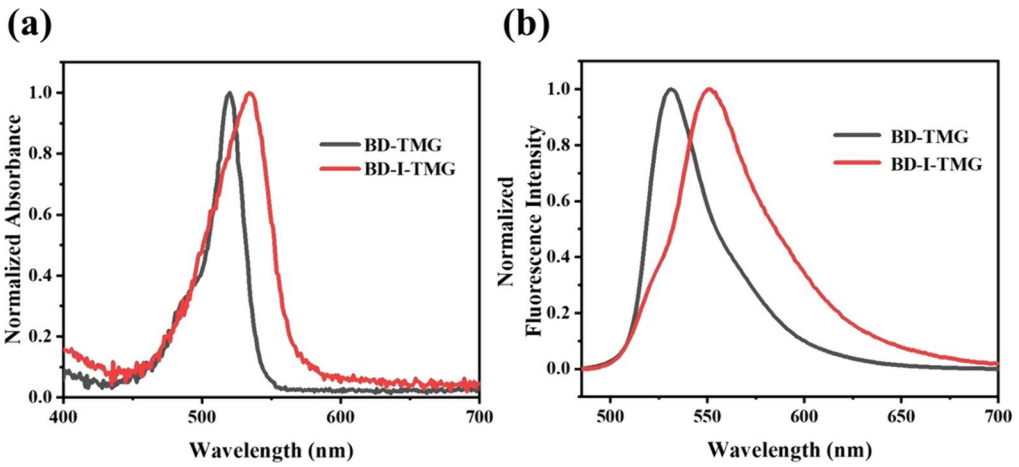

Figure 1. Normalized UV−vis absorption (a) and emission spectra (b, λ_{ex} = 480 nm for BD-TMG and 485 nm for BD-I-TMG) of BD-TMG and BD-I-TMG in CH_2Cl_2.

onate, and trimethylolpropane trimethacrylate were purchased from Sigma-Aldrich. All chemicals were used as received without further purification. ^{1}H NMR (500 MHz) and ^{13}C NMR (126 MHz) spectra were recorded on a 500 MHz Bruker ultrashield spectrometer. Mass spectra were recorded on a high-resolution, Orbitrap Q Exactive mass spectrometer (Thermo Scientific, San Jose, California). UV−vis absorption spectra were obtained on a Tecan Infinite M200 PRO plate reader spectrometer in 1 cm-path-length quartz cuvettes. Fluorescence spectra were recorded on an Edinburgh FLS980 fluorescence spectrometer. FTIR spectra were recorded by using a Shimadzu IRAffinity-1 instrument. The letter mold used for photopolymerization is made of silicone, and the size of each letter is about 0.6 × 0.3 × 0.3 in.

Synthesis of Photobase Generators. *Synthesis and Characterization of BODIPY-OAc.* 2,4-Dimethyl pyrrole (3.00 g, 31.53 mmol) was dissolved in dry CH_2Cl_2 (40 mL) under nitrogen. Acetoxyacetyl chloride (2.58 g, 18.92 mmol) was added to the solution dropwise, and the mixture was stirred at room temperature for 30 min. The solution was then refluxed at 40 °C for 2 h. The solution was cooled to room temperature, and then *N*,*N*-diisopropylethylamine (DIPEA, 8.15 g, 63.06 mmol) was added dropwise. After the mixture was stirred for 1 h, $BF_3{\cdot}OEt_2$ (8.95 g, 63.06 mmol) was added dropwise and the mixture was stirred for another 1 h. After this time, the solvents were partially evaporated and the residue was extracted with CH_2Cl_2 (3 × 20 mL), and then the mixture was washed with brine (2 × 20 mL) and dried over anhydrous Na_2SO_4. The mixture was then evaporated to remove the solvent, and the residue was purified on a silica column using CH_2Cl_2 and hexanes (1:2, v/v), affording BODIPY-OAc as a dark-red solid, as reported in literature[52] (3.120 g, 51.5% yield). ^{1}H NMR (500 MHz, $CDCl_3$) δ (ppm): 6.08 (s, 2H), 5.30 (s, 2H), 2.53 (s, 6H), 2.36 (s, 6H), 2.13 (s, 3H).

Synthesis and Characterization of BODIPY−OH. The synthesis was slightly modified based on a reported method.[32] A mixture of NaOH water solution (13 mL, 0.10 M) and methanol (40 mL) was stirred for 10 min and then added to a solution of BODIPY-OAc (1.00 g, 3.12 mmol) in CH_2Cl_2 (20 mL). The reaction mixture was then stirred overnight in the dark at room temperature. Next, the solvents were partially evaporated and the residue was extracted with CH_2Cl_2 (3 × 20 mL). The combined organic layers were then washed with 1 M HCl (2 × 20 mL) and brine (1 × 20 mL) and dried over anhydrous Na_2SO_4. BODIPY−OH was purified on a silica column using ethyl acetate, CH_2Cl_2, and hexanes (1:18:2, v/v/v), yielding a red precipitate (0.55 g, 63.1% yield). ^{1}H NMR (500 MHz, $CDCl_3$) δ (ppm): 6.24 (s, 2H), 5.54 (s, 1H), 4.73 (s, 2H), 2.51 (s, 6H), 2.42 (s, 6H).

Synthesis and Characterization of BODIPY-I−OH. Similar to a reported method,[53] BODIPY−OH (60 mg, 0.22 mmol) was dissolved in dry tetrahydrofuran (2.5 mL) in dark conditions under nitrogen. A solution of *N*-iodosuccinimide (106 mg, 0.475 mmol) in dry THF (3 mL) was added dropwise to the preceding solution. The mixture was stirred at room temperature for 4 h and evaporated to remove the solvent. The residue was extracted with CH_2Cl_2 (3 × 20 mL), and then the organic layer was washed with brine (2 × 10 mL) and dried over anhydrous Na_2SO_4. BODIPY-I−OH was purified on a silica column using ethyl acetate and CH_2Cl_2 (1:20, v/v), providing a purple solid (53.6 mg, 60% yield). ^{1}H NMR (500 MHz, $CDCl_3$) δ (ppm): 6.17 (s, 1H), 5.33 (s, 1H), 4.95 (s, 2H), 2.64 (s, 3H), 2.57 (s, 3H), 2.55 (d, 6H).

Synthesis and Characterization of BD-TMG. BODIPY−OH (50 mg, 0.18 mmol) and triphosgene (37.3 mg, 0.13 mmol) were added to a cold anhydrous CH_2Cl_2 solution (40 mL, 0 °C). A solution of pyridine (35.6 mg, 0.45 mmol) and anhydrous CH_2Cl_2 (2 mL) was stirred for 2 min and then added to the above solution dropwise. The mixture was stirred for 30 min at 0 °C. Next, a solution of TMG (49.7 mg, 0.43 mmol) and anhydrous CH_2Cl_2 was stirred for 2 min and then added to the above mixture. The reaction mixture was stirred overnight at room temperature. After this, the solvent was carefully evaporated and the residue was washed with brine (3 × 30 mL). The organic layer was dried over anhydrous Na_2SO_4 and purified by silica gel chromatography with CH_3OH and CH_2Cl_2 (1:20, v/v), affording BODIPY-TMG as a dark-purple solid (21 mg, 28% yield). ^{1}H NMR (500 MHz, $CDCl_3$) δ (ppm): 6.05 (s, 2H), 5.25 (s, 2H), 2.88 (s, 12 H), 2.52 (s, 6H), 2.44 (s. 6H). ^{13}C NMR (126 MHz, $CDCl_3$) δ (ppm): 166.65, 159.75, 155.74, 155.59, 141.75, 135.46, 121.84, 121.77, 58.13, 39.89, 15.62, 14.64. HRMS (ESI+) calcd for $[M + H]^+$ ($C_{20}H_{29}BF_2N_5O_2$) 420.23769; found 420.23828.

Synthesis and Characterization of BD-I-TMG. BODIPY-I−OH (50 mg, 0.12 mmol) and triphosgene (36.7 mg, 0.12 mmol) were added to a cold anhydrous DCM solution (40 mL, 0 °C). The solution of pyridine (29.4 mg, 0.37 mmol) and anhydrous DCM (2 mL) was stirred for 2 min and then added to the above solution dropwise. The mixture was stirred for 30 min at 0 °C. Next, a solution of TMG (42.8 mg, 0.37 mmol) and anhydrous DCM was stirred for 2 min and then added to the above mixture. The reaction mixture was stirred overnight at room temperature. After this, the solvent was carefully evaporated and the residue was washed with brine (3 × 30 mL). The organic layer was dried over anhydrous Na_2SO_4 and purified by silica gel chromatography with CH_3OH and CH_2Cl_2 (1:20, v/v). BODIPY-I-TMG as the final product (21 mg, 31% yield). ^{1}H NMR (500 MHz, $CDCl_3$) δ (ppm): 6.10 (s, 1H), 5.24 (s, 2H), 2.88 (s, 12H), 2.58 (s, 3H), 2.52 (s, 3H), 2.45 (d, 6H). ^{13}C NMR (126 MHz, $CDCl_3$) δ (ppm): 166.74, 159.62, 158.37, 154.64, 143.88, 141.56, 135.30, 133.62, 132.20, 123.08, 58.28, 39.94, 29.72, 17.71, 15.98. HRMS (ESI+) calcd for $[M + H]^+$ ($C_{20}H_{28}BF_2IN_5O_2$) 546.13433; found 546.13460.

https://doi.org/10.1021/acsami.3c09326
ACS Appl. Mater. Interfaces 2023, 15, 45281−45289

Table 1. Photophysical Properties of BD-TMG and BD-I-TMG

	λ_{max}^{abs} (nm)[a]	λ_{max}^{em} (nm)[b]	ε (10^4 M^{-1} cm^{-1})[c]	Φ_f[d]	τ (ns)[e]	Φ_{TMG}[f]	$\varepsilon\Phi_{TMG}$ (M^{-1} cm^{-1})
BD-TMG	520	531	5.69 ± 0.173	0.84	4.37	0.009	512.1
BD-I-TMG	535	551	3.13 ± 0.12	0.09	0.66	0.029	907.7

[a]Wavelength of maximum absorption. [b]Wavelength of maximum emission. [c]Extinction coefficient. [d]Fluorescence quantum yield (error in measurement ±1.2%). [e]Fluorescence lifetimes (error in measurement ≤10 ps). [f]Photobase generation quantum yield (error in measurement ±2.9%).

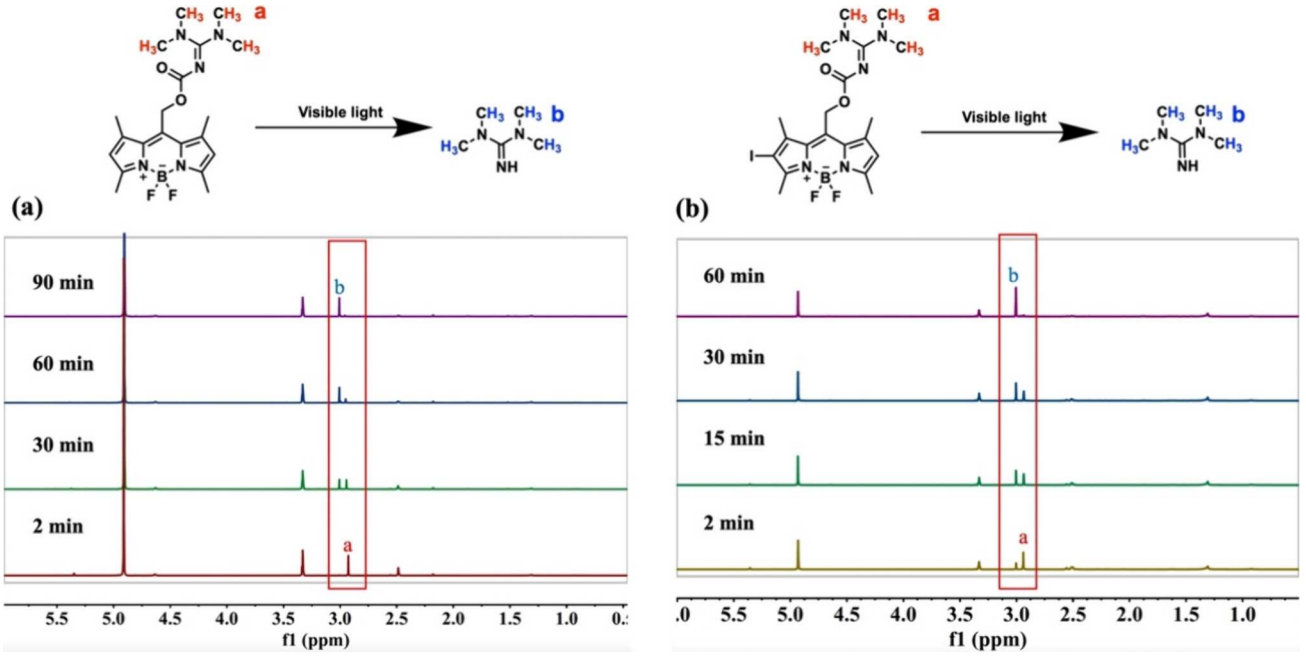

Figure 2. BD-I-TMG (a) and BD-TMG (b) photo degradation in CD_3OD. The samples were irradiated by Thorlabs M505L3 LED light source (nominal wavelength 505 nm, power density is 80 mW/cm^2, samples were concentrated for ^{1}H NMR measurements).

RESULTS AND DISCUSSION

The synthesis began with the preparation of the BODIPY core with an ester at the meso-position (BODIPY-OAc) by reacting 2,4-dimethyl pyrrole with acetoxyacetyl chloride. Then, the ester was hydrolyzed to liberate the hydroxyl group for postmodification in the following steps. The hydrolysis procedure was modified based on a reported protocol.[32] To introduce a heavy atom to the BODIPY core, NIS was used in THF in the dark as the iodination agent to add an iodine atom to the BODIPY core at position 2 (Scheme 1). When compared to other heavy atoms, such as bromine and chlorine, iodine can greatly enhance the spin−orbit coupling that results in an efficient intersystem crossing rate.[53,54] At this stage, we obtained two photocages, BD−OH and BD-I−OH, which were further conjugated with TMG to realize photolysis and photobase release.

In the last step, we attempted to use the transesterification mechanism to convert the alcohol of BD−OH and BD-I−OH into ester through carbonyldiimidazole (CDI) under the catalysis of the DMAP.[30] However, we rarely obtained the final product via this synthetic route. We then tried to convert the alcohol of BD−OH and BD-I−OH into chloroformate with triphosgene and then used it to react with the amino group of TMG to give the final products. Here, we first reported a method to conjugate TMG with BODIPY esters by amidation. This approach provides a high yield and high reaction rate, such that BD−OH and BD-I−OH were obtained separately as dark-red and dark-purple solids with reasonable yields of 28 and 31%, respectively. It is worth noting that the preparation of the derivative with diiodine failed using a similar synthetic approach.

The photophysical properties of BD-TMG and BD-I-TMG were then investigated by UV−vis absorption and steady-state fluorescence emission spectroscopy (Figure 1). The absorption spectra of BD-TMG and BD-I-TMG showed an intense peak centered at 520 and 535 nm, respectively, and the emission was located at 531 and 551 nm, respectively. Furthermore, the molar absorptivity values (ε) of BD-TMG and BD-I-TMG were 5.69×10^4 and 3.13×10^4 M^{-1} cm^{-1}. Compared with BD-TMG, BD-I-TMG exhibited a red-shifted absorbance, emission, and maximum absorptivity, which is similar to literature reports.[32,52] The fluorescence quantum yields (Φ_f) were measured in dichloromethane and calculated using Rhodamine 6G as the standard. The fluorescence quantum yield, Φ_f, values for BD-TMG and BD-I-TMG in CH_2Cl_2 were 0.84 and 0.09, respectively (Table 1). Moreover, the fluorescence lifetime (τ) of BD-I-TMG exhibited an obvious decrease compared to that of BD-TMG, consistent with a heavy atom effect from the iodination of the BODIPY core causing quenching of fluorescence by increasing the intersystem crossing (ISC) from the first excited singlet to the triplet state.

Before studying the release of TMG under light irradiation, we first explored the stability of our PBGs under dark conditions. The results showed that after 24 h in the dark, both BD-TMG and BD-I-TMG have a negligible change in their

https://doi.org/10.1021/acsami.3c09326
ACS Appl. Mater. Interfaces 2023, 15, 45281−45289

Scheme 2. Possible Pathway for the Photolysis of Photocaged TMG

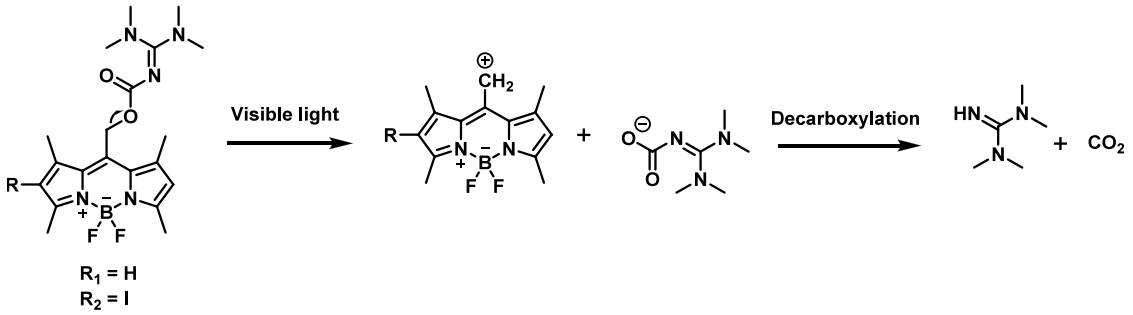

Table 2. Scope of Photo Thiol−Ene Michael Addition Catalyzed by BD-TMG and BD-I-TMG

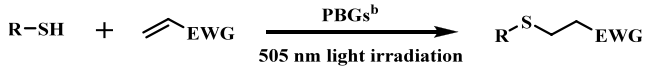

entry	thiol	vinyl	catalyst	yield[a](%)
1	butyl thioglycolate	ethyl acrylate	BD-TMG	63
2	butyl 3-mercaptopropionate	divinyl sulfone	BD-TMG	94
3	butyl thioglycolate	divinyl sulfone	BD-TMG	68
4	butyl 3-mercaptopropionate	ethyl acrylate	BD-TMG	98
5	butyl thioglycolate	ethyl acrylate	BD-I-TMG	98
6	butyl 3-mercaptopropionate	divinyl sulfone	BD-I-TMG	95
7	butyl thioglycolate	divinyl sulfone	BD-I-TMG	76
8	butyl 3-mercaptopropionate	ethyl acrylate	BD-I-TMG	96

[b]Reaction conditions: thiol (1 mmol), vinyl (1 mmol), and PBGs (2.5 mol %) irradiated using a 505 nm LED light source (power density is 80 mW/cm^2, irradiated distance: 1 cm) for 30 min. [a]Reaction yields are determined by ^{1}H NMR.

UV−vis spectra, indicating high dark stability (as shown in Figure S12). In addition, we also verified the stability with increased temperature and found that our compounds were stable even at 60 °C (as shown in Figure S11).

Furthermore, to show that these structures can release TMG under green-light irradiation, we investigated the photolysis process of BD-TMG and BD-I-TMG by monitoring the reaction with ^{1}H NMR. The PBGs were dissolved in CD_3OD. A 400 mW, 505 nm LED lamp was used to irradiate the sample (irradiance: 80 mW/cm^2) and the irradiation-time-dependent ^{1}H NMR spectra were recorded (Figure 2). With increasing irradiation time, the peak around 2.9 ppm decreased, which corresponds to the methyl groups of TMG of BD-TMG and BD-I-TMG. This decreasing peak results from the photolysis process of the carbamate group on BD-TMG and BD-I-TMG. At the same time, the peak from free TMG at 3.01 ppm increases gradually. More importantly, the TMG releasing speed of BD-I-TMG is much faster than that of BD-TMG, with more TMG released within the first 2 min, and fully released TMG in the period of 60 min light irradiation. This also supports the heavy atom effect, in which the iodine in BD-I-TMG can enhance ISC and facilitate conversion from the singlet state to the triplet state. Furthermore, as reported in the literature,[52] BODIPY-based PBGs' carbamate cleavage relaxation mainly occurred from the T_1 state, implying that iodination can improve the deprotection efficiency of TMG. The photolytic efficiency tests substantiated this. To further investigate the role of triplet states on the photoreleasing process, the Stern−Volmer quenching experiment was utilized. Photolysis of 1×10^{-5} M BD-I-TMG in dichloromethane was irradiated with or without the addition of 5 mM triplet quencher potassium sorbate (PS).[55] A significantly slower photolysis rate was observed using UV−vis when PS was introduced, confirming that the improved TMG releasing efficiency is facilitated by the heavy atom effect (Figure S10). Moreover, we also studied the effect of oxygen in the solvent on the photolysis rate of BD-I-TMG. 1×10^{-5} M BD-I-TMG in degassed dichloromethane was prepared for the photolysis analysis. The irradiation time-dependent photolysis was monitored by UV−vis (Figure S10). The results showed that the rate of photolysis of BD-I-TMG in the degassed solvent was slightly higher than in the nondegassed solvent, indicating the energy transfer from triplet states to oxygen. However, the difference was minor and nondegassed conditions were used in the experiments below.

The photobase generation quantum yield of BD-I-TMG (Φ_{TMG} = 0.029) and photolytic efficiency ($\varepsilon\Phi_{TMG}$ = 907.7) were superior to those of the BD-TMG (Φ_{TMG} = 0.009, $\varepsilon\Phi_{TMG}$ = 512.1) system. Moreover, the photolytic efficiency of BD-I-TMG is much greater than traditional *o*-nitrobenzyl-based PBGs[24] and the quantum yield is close to the coumarin-based PBGs.[30] In addition, we observed a significant decrease in the photolysis rate when aprotic $CDCl_3$ was used (as shown in Figure S13) as the solvent. This result indicates that the nucleophilic solvent (e.g., CH_3OH) facilitates the photodecomposition rate. Additionally, to confirm this photolysis process, time-dependent UV−vis measurements were used. As expected, under 505 nm light irradiation, a decrease in the peaks at 520 and 535 nm of BD-TMG and BD-I-TMG were observed, respectively (as shown in Figure S9).

We postulate that the photolysis mechanism of BD-TMG and BD-I-TMG proceeds as described in Scheme 2. A similar photoheterolysis mechanism was reported by Winter et al. with similar BODIPY cage structures.[56] Under visible-light irradiation, the BODIPY-based photocages were excited to the singlet and triplet states. A photocleavage process ensued,

https://doi.org/10.1021/acsami.3c09326
ACS Appl. Mater. Interfaces 2023, 15, 45281−45289

where the C−O bond broke and produced the BODIPY methyl cation and the corresponding anion leaving group. Among them, the BODIPY methyl cation group was restabilized by nucleophiles such as MeOH while the carbamate anion underwent the decarboxylation process to produce tetramethylguanidine (TMG) and CO_2. To further study the photodegradation process and photolysis products of BD-TMG, we used ^{1}H NMR to monitor the mixture after green light irradiation (80 mW/cm^2, 505 nm LED light for 2 and 60 min; Figure S14). ^{1}H NMR showed that a peak at 5.53 ppm increases with irradiation time, which corresponds to the OH after the carbocation intermediate reacts with H_2O in the solvent. Moreover, the CH_2 peak shifted from 5.32 to 4.72 ppm, indicating that the environment changes from an ester and an alcohol after TMG release. It is worth mentioning that the basicity of protected TMG and free TMG is significantly different[57] to allow the regulation of thiol−ene Michael addition reactions.

To further explore the activation activity of BD-TMG and BD-I-TMG toward the thiol−ene Michael reaction, different monothiols were evaluated with ethyl acrylate and divinyl sulfone separately as model substrates. The light source used was Thorlab's M505L3 (nominal wavelength is 505 nm with an irradiance of 80 mW/cm^2, irradiated distance: 1 cm). The reaction yields were determined by ^{1}H NMR. 2.5 mol % yield of photobase generators was found to be efficient for the reaction (Figure S15), and Table 2 includes the results, which indicate that using a 2.5 mol % catalyst loading of BD-TMG or BD-I-TMG showed high catalyst efficiency, and all the entries' reaction conversions were completed in 30 min. The result shows that the activation of the thiol−ene additions with BD-I-TMG has a higher yield than BD-TMG. This result can be attributed to the BD-I-TMG having much higher photolysis efficiency than BD-TMG. In addition, by comparing the reaction yield after 30 min of irradiation, both BD-TMG entries and BD-I-TMG were close to 100%, which indicated that 2.5 mol % of catalyst loading is in excess for the 1 mmol of thiol and ene.

To examine the kinetics of the photoactivation of the thiol−ene Michael reaction, BD-TMG and BD-I-TMG were implemented as photoactivators in the butyl thioglycolate and ethyl acrylate reactions under continuous visible-light irradiation (505 nm, 80 mW/cm^2). The thiol conversion was monitored by FTIR spectroscopy (Figure 3), monitoring the reduction of peak intensity around 2650 cm^{-1}, which corresponds to the thiol group of butyl thioglycolate. The final thiol conversion yield was confirmed by ^{1}H NMR.

In Figure 3, the results indicate that both BD-TMG and BD-I-TMG exhibited fast reaction kinetics; however, the reaction rate of BD-I-TMG was higher than that of BD-TMG during the first 2.5 min of irradiation. In addition, the final thiol conversion of BD-I-TMG (ca. 85%) was also higher than that of BD-TMG (65%) under 20 min of continuous irradiation. Furthermore, it was shown that the PBGs and visible-light irradiation are both necessary to initiate the thiol−ene Michael reaction. In the absence of either PBGs or green light, no apparent reaction was observed. In addition, we also conducted the dark cure test for BD-TMG and BD-I-TMG. The model reaction mixture was irradiated with LED light for 2.5 min, and the thiol conversion was monitored in the dark using FTIR (as shown in Figure S19). The result showed that BD-TMG and BD-I-TMG have the ability for dark cure, but the reaction rate after 2.5 min irradiation was slower than in continuous irradiation trials.

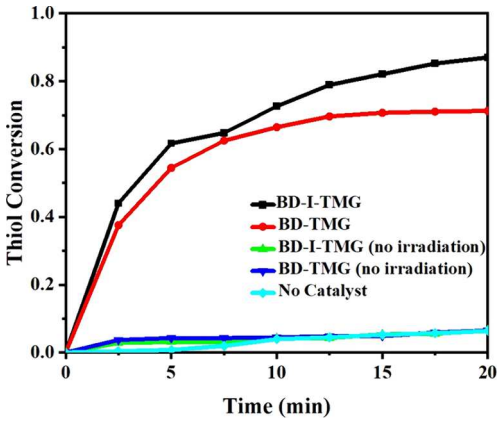

Figure 3. Thiol conversion versus time monitored by FTIR for the model reaction between butyl thioglycolate and ethyl acrylate with 2.5 mol % photocatalyst loading. Light source: Thorlabs M505L3 LED light (nominal wavelength 505 nm, power density 80 mW/cm^2, irradiated distance: 1 cm).

To demonstrate the utility of the BODIPY PBGs, a photopolymerization study was conducted. To form a polymer network, we implemented BD-I-TMG as the photoactivator. A mixture of pentaerythritol tetrakis(mercaptoacetate) (PETMA 1 mmol), trimethylolpropane trimethacrylate (TMPTMA 1 mmol), and 2.5 mol % of BD-I-TMG were well mixed and placed in a rubber mold. We noticed the complete sol−gel transition after 1 h green-light irradiation using a vial inversion test (as shown in Figure S17b). After 1 h of 505 nm LED light (80 mW/cm^2) irradiation, a soft rubbery polymer was obtained (Figure 4), which indicated that BD-I-TMG successfully initiated the polymerization reaction and formed cross-linked polymers during the photopolymerization process. Using this approach, 10 mm-thick polymers can be prepared without dark cure (as shown in Figure S17a). Finally, to assess the mechanical properties of the polymer, the 0.5 mm-thick film made of a stoichiometric mixture of PETMP and TMPTMA

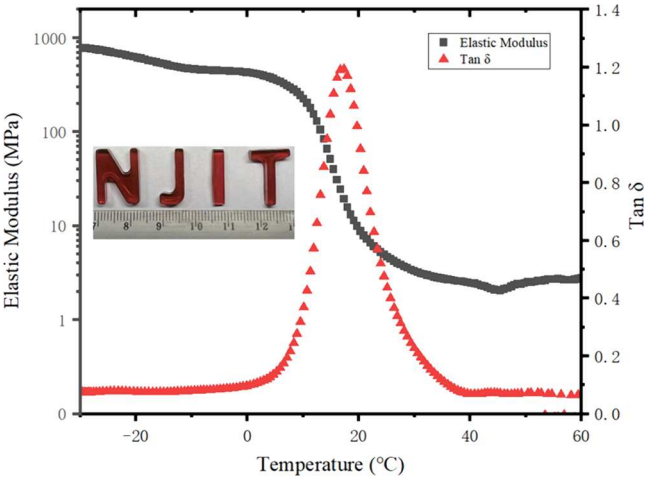

Figure 4. Plots of tan δ and elastic modulus vs temperature for polymer networks formed through the monomer cross-linking PETMP/TMPTMA (molar ratio = 1:1) and 2.5 mol % BD-I-TMG catalyst loading. The sample was irradiated with 80 mW/cm^2, 505 nm LED light for 1 h. The irradiation distance is 1 cm.

https://doi.org/10.1021/acsami.3c09326
ACS Appl. Mater. Interfaces 2023, 15, 45281−45289

(molar ratio = 1:1) was cured in the presence of 2.5 mol % BD-I-TMG and tested via dynamic mechanical analysis (DMA) experiments (as shown in Figure 4). Both the glass transition temperature (T_g = 17.36 °C) and narrow tan δ indicated the formation of a homogeneous polymer network under the activation of BD-I-TMG and green LED light. In addition, we also evaluated rheological and mechanical properties of the BD-I-TMG-catalyzed cross-linked sample (Figure S18). The compressive modulus values obtained from compression tests were 11.9 ± 2.8 MPa (Figure S18A). The frequency sweep results confirm that the polymer is cross-linked and well structured, as the storage modulus (G') values were higher than the loss modulus (G'') values over a wide range of frequencies (Figure S18B).

CONCLUSIONS

In summary, two novel BODIPY-based TMG-protected photobase generators, BD-TMG and BD-I-TMG, have been successfully synthesized for green-light-initiated thiol−ene Michael addition photopolymerization. Both the PBGs' photophysical properties and photolysis efficiencies were studied. These two PBGs exhibited a long-wavelength-absorption ability in the visible-wavelength window above 500 nm. Compared with BD-TMG, the heavy atom (iodine)-labeled BODIPY derivative, BD-I-TMG, had much greater photoreleasing efficiency resulting from the heavy atom effect. Furthermore, the model Michael reactions of different thiols and enes were evaluated. BD-I-TMG was a very effective photocatalyst, displaying a higher $\varepsilon\Phi_{TMG}$ value. BD-I-TMG was also employed to prepare a cross-linked polymer whose mechanical properties were characterized and indicated a resulting relatively homogeneous network. The results demonstrated that BD-I-TMG has the ability of spatial and temporal control over the release of TMG and can successfully initiate the polymerization via the thiol−ene Michael reaction and form a homogeneous polymer network. Due to the flexibility of the BODIPY structure, there is great potential to further extend the conjugation and achieve far red light-triggered photopolymerization for biomedical applications and wavelength orthogonal control.[58] Overall, this work opens the possibility of using a PBG to induce thiol−ene Michael reactions at longer visible wavelengths with high photocatalyst efficiency in a number of applications ranging from biomaterials to structural materials.

ASSOCIATED CONTENT

Supporting Information

The Supporting Information is available free of charge at https://pubs.acs.org/doi/10.1021/acsami.3c09326.

NMR and mass spectra of BD-TMG and BD-I-TMG; photophysical properties of BD-TMG and BD-I-TMG; photochemical properties and stabilities of PBGs; BD-TMG photo degradation evaluation in $CDCl_3$; Fourier transform infrared spectroscopy (FTIR); dynamic mechanical analysis (DMA); and rheological and mechanical characterization (PDF)

AUTHOR INFORMATION

Corresponding Authors

Kevin D. Belfield − *Department of Chemistry and Environmental Science, College of Science and Liberal Arts, New Jersey Institute of Technology, Newark, New Jersey 07102, United States;* orcid.org/0000-0002-7339-2813; Email: Belfield@njit.edu

Yuanwei Zhang − *Department of Chemistry and Environmental Science, College of Science and Liberal Arts, New Jersey Institute of Technology, Newark, New Jersey 07102, United States;* orcid.org/0000-0003-2111-0981; Email: yuanwei.zhang@njit.edu

Authors

Shupei Yu − *Department of Chemistry and Environmental Science, College of Science and Liberal Arts, New Jersey Institute of Technology, Newark, New Jersey 07102, United States*

Ojasvita Reddy − *Department of Chemistry and Environmental Science, College of Science and Liberal Arts, New Jersey Institute of Technology, Newark, New Jersey 07102, United States*

Alperen Abaci − *Otto H. York Department of Chemical and Materials Engineering, New Jersey Institute of Technology, Newark, New Jersey 07102, United States*

Yongling Ai − *Department of Chemistry and Environmental Science, College of Science and Liberal Arts, New Jersey Institute of Technology, Newark, New Jersey 07102, United States;* orcid.org/0000-0003-4458-2041

Yanmei Li − *Department of Chemistry and Environmental Science, College of Science and Liberal Arts, New Jersey Institute of Technology, Newark, New Jersey 07102, United States*

Hao Chen − *Department of Chemistry and Environmental Science, College of Science and Liberal Arts, New Jersey Institute of Technology, Newark, New Jersey 07102, United States;* orcid.org/0000-0001-8090-8593

Murat Guvendiren − *Otto H. York Department of Chemical and Materials Engineering, New Jersey Institute of Technology, Newark, New Jersey 07102, United States*

Complete contact information is available at: https://pubs.acs.org/10.1021/acsami.3c09326

Notes

The authors declare no competing financial interest.

ACKNOWLEDGMENTS

We wish to acknowledge support from the New Jersey Health Foundation (PC 57-20 and PC 25-22). K.D.B. acknowledges support from the US National Science Foundation (CHE-1726345), the National Institute of Health (R21AA028340), and the Becton-Dickinson Research Professorship. This work is partially funded by the National Science Foundation (NSF) CAREER award grant number 2044479 (M.G.). O.R. acknowledges support from the NSF BioSMART REU program and NJIT Undergraduate Research & Innovation program.

REFERENCES

(1) Kolb, H. C.; Finn, M. G.; Sharpless, K. B. Click Chemistry: Diverse Chemical Function from a Few Good Reactions. *Angew. Chem., Int. Ed.* **2001**, *40* (11), 2004−2021.

(2) Nair, D. P.; Podgórski, M.; Chatani, S.; Gong, T.; Xi, W.; Fenoli, C. R.; Bowman, C. N. The Thiol-Michael Addition Click Reaction: a Powerful and Widely Used Tool in Materials Chemistry. *Chem. Mater.* **2014**, *26* (1), 724−744.

(3) Chatani, S.; Gong, T.; Earle, B. A.; Podgorski, M.; Bowman, C. N. Visible-Light Initiated Thiol-Michael Addition photopolymerization Reactions. *ACS Macro Lett.* **2014**, *3* (4), 315−318.
(4) Sutherland, B. P.; Kabra, M.; Kloxin, C. J. Expanding the Thiol-X Toolbox: Photoinitiation and Materials Application of the Acid-Catalyzed Thiol-ene (ACT) Reaction. *Polym. Chem.* **2021**, *12* (10), 1562−1570.
(5) Kumar, R.; Santa Chalarca, C. F.; Bockman, M. R.; Bruggen, C. V.; Grimme, C. J.; Dalal, R. J.; Hanson, M. G.; Hexum, J. K.; Reineke, T. M. Polymeric Delivery of Therapeutic Nucleic Acids. *Chem. Rev.* **2021**, *121* (18), 11527−11652.
(6) Najafi, F.; Salami-Kalajahi, M.; Roghani-Mamaqani, H. Synthesis of Amphiphilic Janus Dendrimer and its Application in Improvement of Hydrophobic Drugs Solubility in Aqueous Media. *Eur. Polym. J.* **2020**, *134*, 109804.
(7) Pashaei-Sarnaghi, R.; Najafi, F.; Taghavi-Kahagh, A.; Salami-Kalajahi, M.; Roghani-Mamaqani, H. Synthesis, Photocrosslinking, and Self-Assembly of Coumarin-Anchored Poly(amidoamine) Dendrimer for Smart Drug Delivery System. *Eur. Polym. J.* **2021**, *158*, 110686.
(8) Li, H.; Tang, S.; Zhou, Q.; Chen, W.; Yang, X.; Xing, T.; Zhao, Y.; Chen, G. Durable Superhydrophobic Cotton Fabrics Prepared by Surface-Initiated Electrochemically Mediated ATRP of Polyhedral Vinylsilsesquioxane and Subsequent Fluorination via Thiol-Michael Addition Reaction. *J. Colloid Interface Sci.* **2021**, *593*, 79−88.
(9) Reese, C. M.; Thompson, B. J.; Logan, P. K.; Stafford, C. M.; Blanton, M.; Patton, D. L. Sequential and One-Pot Post-Polymerization Modification Reactions of Thiolactone-Containing Polymer Brushes. *Polym. Chem.* **2019**, *10* (36), 4935−4943.
(10) Yee, D. W.; Schulz, M. D.; Grubbs, R. H.; Greer, J. R. Functionalized 3D Architected Materials via Thiol-Michael Addition and Two-Photon Lithography. *Adv. Mater.* **2017**, *29* (16), 1605293.
(11) Berry, D. R.; Díaz, B. K.; Durand-Silva, A.; Smaldone, R. A. Radical Free Crosslinking of Direct-Write 3D Printed Hydrogels through a Base Catalyzed Thiol-Michael Reaction. *Polym. Chem.* **2019**, *10* (44), 5979−5984.
(12) Rossegger, E.; Höller, R.; Hrbinič, K.; Sangermano, M.; Griesser, T.; Schlögl, S. 3D Printing of Soft Magnetoactive Devices with Thiol-Click Photopolymer Composites. *Adv. Eng. Mater.* **2023**, *25*, 2200749.
(13) Zhang, Y.; Li, X.; Zhu, Q.; Wei, W.; Liu, X. Photocurable hyperbranched Polymer Medical Glue for Water-Resistant Bonding. *Biomacromolecules* **2020**, *21* (12), 5222−5232.
(14) Daglar, O.; Gungor, B.; Guric, G.; Gunay, U. S.; Hizal, G.; Tunca, U.; Durmaz, H. Rapid hyperbranched Polythioether Synthesis Through Thiol-Michael Addition Reaction. *J. Polym. Sci.* **2020**, *58* (6), 824−830.
(15) Sinha, J.; Soars, S.; Bowman, C. N. Enamine Organocatalysts for the Thiol-Michael Addition Reaction and Cross-Linking Polymerizations. *Macromolecules* **2021**, *54* (4), 1693−1701.
(16) McNair, O. D.; Brent, D. P.; Sparks, B. J.; Patton, D. L.; Savin, D. A. Sequential Thiol Click Reactions: Formation of Ternary Thiourethane/thiol-ene Networks with Enhanced Thermal and Mechanical Properties. *ACS Appl. Mater. Interfaces* **2014**, *6* (9), 6088−97.
(17) Fouassier, J.-P.; Lalevée, J. *photoinitiators for Polymer Synthesis: Scope, Reactivity, and Efficiency*; Wiley-VCH: Weinheim, 2012.
(18) Kaneko, Y.; Sarker, A. M.; Neckers, D. C. Mechanistic Studies of Photobase Generation from Ammonium Tetraorganyl Borate Salts. *Chem. Mater.* **1999**, *11* (1), 170−176.
(19) Tachi, H.; Shirai, M.; Tsunooka, M. Technology, Photolysis of Quaternary Ammonium Dithiocarbamates and their Use as Photobase Generators. *J. Photopolym. Sci. Technol.* **2000**, *13* (1), 153−156.
(20) Salmi, H.; Allonas, X.; Ley, C.; Defoin, A.; Ak, A. Quaternary Ammonium Salts of Phenylglyoxylic Acid as Photobase Generators for Thiol-Promoted Epoxide photopolymerization. *Polym. Chem.* **2014**, *5* (22), 6577−6583.
(21) Zhang, X.; Wang, X.; Chatani, S.; Bowman, C. N. Phosphonium Tetraphenylborate: A photocatalyst for Visible-Light-Induced, Nucleophile-Initiated Thiol-Michael Addition photopolymerization. *ACS Macro Lett.* **2021**, *10* (1), 84−89.
(22) Zivic, N.; Sadaba, N.; Almandoz, N.; Ruipérez, F.; Mecerreyes, D.; Sardon, H. Thioxanthone-Based Photobase Generators for the Synthesis of Polyurethanes via the photopolymerization of Polyols and Polyisocyanates. *Macromolecules* **2020**, *53* (6), 2069−2076.
(23) Xi, W.; Peng, H.; Aguirre-Soto, A.; Kloxin, C. J.; Stansbury, J. W.; Bowman, C. N. Spatial and Temporal Control of Thiol-Michael Addition via photocaged Superbase in Photopatterning and Two-Stage Polymer Networks Formation. *Macromolecules* **2014**, *47* (18), 6159−6165.
(24) Zhang, X.; Xi, W.; Gao, G.; Wang, X.; Stansbury, J. W.; Bowman, C. N. *o*-Nitrobenzyl-Based Photobase Generators: Efficient photoinitiators for Visible-Light Induced Thiol-Michael Addition photopolymerization. *ACS Macro Lett.* **2018**, *7* (7), 852−857.
(25) Zivic, N.; Kuroishi, P. K.; Dumur, F.; Gigmes, D.; Dove, A. P.; Sardon, H. Recent Advances and Challenges in the Design of Organic photoacid and Photobase Generators for Polymerizations. *Angew. Chem., Int. Ed.* **2019**, *58* (31), 10410−10422.
(26) Suyama, K.; Fuke, K.; Yamamoto, T.; Kurokawa, Y.; Tsunooka, M.; Shirai, M. Photochemical Formation of Ammonium/thiolate Complexes from Quaternary Ammonium Thiocyanates and its Use in Crosslinking of Polymers. *J. Photochem. Photobiol. A: Chem.* **2006**, *179* (1−2), 87−94.
(27) Klán, P.; Šolomek, T.; Bochet, C. G.; Blanc, A.; Givens, R.; Rubina, M.; Popik, V.; Kostikov, A.; Wirz, J. Photoremovable Protecting Groups in Chemistry and Biology: Reaction Mechanisms and Efficacy. *Chem. Rev.* **2013**, *113* (1), 119−191.
(28) Hillel, A. T.; Unterman, S.; Nahas, Z.; Reid, B.; Coburn, J. M.; Axelman, J.; Chae, J. J.; Guo, Q.; Trow, R.; Thomas, A.; Hou, Z.; Lichtsteiner, S.; Sutton, D.; Matheson, C.; Walker, P.; David, N.; Mori, S.; Taube, J. M.; Elisseeff, J. H. Photoactivated Composite Biomaterial for Soft Tissue Restoration in Rodents and in Humans. *Sci. Transl. Med.* **2011**, *3* (93), 93ra67.
(29) Karami, P.; Rana, V. K.; Zhang, Q.; Boniface, A.; Guo, Y.; Moser, C.; Pioletti, D. P. NIR Light-Mediated Photocuring of Adhesive Hydrogels for Noninvasive Tissue Repair via Upconversion Optogenesis. *Biomacromolecules* **2022**, *23* (12), 5007−5017.
(30) Zhang, X.; Xi, W.; Wang, C.; Podgorski, M.; Bowman, C. N. Visible-Light-Initiated Thiol-Michael Addition Polymerizations with Coumarin-Based Photobase Generators: Another Photoclick Reaction Strategy. *ACS Macro Lett.* **2016**, *5* (2), 229−233.
(31) Engelke, J.; Truong, V. X. Visible Light Enabled para-Fluoro-Thiol Ligation. *Polym. Chem.* **2020**, *11* (44), 7015−7019.
(32) Sitkowska, K.; Feringa, B. L.; Szymanski, W. Green-Light-Sensitive BODIPY photoprotecting Groups for Amines. *J. Org. Chem.* **2018**, *83* (4), 1819−1827.
(33) Wijesooriya, C. S.; Peterson, J. A.; Shrestha, P.; Gehrmann, E. J.; Winter, A. H.; Smith, E. A. A Photoactivatable BODIPY Probe for Localization-Based Super-Resolution Cellular Imaging. *Angew. Chem., Int. Ed.* **2018**, *57* (39), 12685−12689.
(34) Sambath, K.; Liu, X.; Wan, Z.; Hutnik, L.; Belfield, K. D.; Zhang, Y. Potassium Ion Fluorescence Probes: Structures, Properties and Bioimaging. *ChemPhotoChem.* **2021**, *5* (4), 317−325.
(35) Yeh, S. C. A.; Hou, J.; Wu, J. W.; Yu, S.; Zhang, Y.; Belfield, K. D.; Camargo, F. D.; Lin, C. P. Quantification of Bone Marrow Interstitial pH and Calcium Concentration by Intravital Ratiometric Imaging. *Nat. Commun.* **2022**, *13* (1), 393.
(36) Zhang, X.; Xiao, Y.; Qi, J.; Qu, J.; Kim, B.; Yue, X.; Belfield, K. D. Long-Wavelength, Photostable, Two-Photon Excitable BODIPY Fluorophores Readily Modifiable for Molecular Probes. *J. Org. Chem.* **2013**, *78* (18), 9153−9160.
(37) Sui, B.; Bondar, M. V.; Anderson, D.; Rivera-Jacquez, H. J.; Masunov, A. M. E.; Belfield, K. D. New Two-Photon Absorbing BODIPY-Based Fluorescent Probe: Linear Photophysics, Stimulated Emission, and Ultrafast Spectroscopy. *J. Phys. Chem. C* **2016**, *120* (26), 14317−14329.

https://doi.org/10.1021/acsami.3c09326
ACS Appl. Mater. Interfaces 2023, 15, 45281−45289

(38) Li, W.; Xie, Z.; Jing, X. BODIPY Photocatalyzed Oxidation of Thioanisole under Visible Light. *Catal. Commun.* **2011**, *16* (1), 94−97.
(39) Sambath, K.; Wan, Z.; Wang, Q.; Chen, H.; Zhang, Y. BODIPY-Based photoacid Generators for Light-Induced Cationic Polymerization. *Org. Lett.* **2020**, *22* (3), 1208−1212.
(40) Digby, E. M.; Ayan, S.; Shrestha, P.; Gehrmann, E. J.; Winter, A. H.; Beharry, A. A. photocaged DNA-Binding Photosensitizer Enables Photocontrol of Nuclear Entry for Dual-Targeted Photodynamic Therapy. *J. Med. Chem.* **2022**, *65* (24), 16679−16694.
(41) Kim, B.; Sui, B.; Yue, X.; Tang, S.; Tichy, M. G.; Belfield, K. D. In Vitro Photodynamic Studies of a BODIPY-Based Photosensitizer. *Eur. J. Org. Chem.* **2017**, *2017* (1), 25−28.
(42) Kowada, T.; Maeda, H.; Kikuchi, K. BODIPY-Based Probes for the Fluorescence Imaging of Biomolecules in Living Cells. *Chem. Soc. Rev.* **2015**, *44* (14), 4953−4972.
(43) Ulrich, G.; Ziessel, R.; Harriman, A. The Chemistry of Fluorescent BODIPY Dyes: Versatility Unsurpassed. *Angew. Chem., Int. Ed.* **2008**, *47* (7), 1184−1201.
(44) Ni, Y.; Wu, J. Far-red and Near Infrared BODIPY Dyes: Synthesis and Applications for Fluorescent pH Probes and Bio-Imaging. *Org. Biomol. Chem.* **2014**, *12* (23), 3774−3791.
(45) Kand, D.; Liu, P.; Navarro, M. X.; Fischer, L. J.; Rousso-Noori, L.; Friedmann-Morvinski, D.; Winter, A. H.; Miller, E. W.; Weinstain, R. Water-Soluble BODIPY photocages with Tunable Cellular Localization. *J. Am. Chem. Soc.* **2020**, *142* (11), 4970−4974.
(46) Sui, B.; Tang, S.; Woodward, A. W.; Kim, B.; Belfield, K. D. A BODIPY-Based Water-Soluble Fluorescent Probe for Mitochondria Targeting. *Eur. J. Org. Chem.* **2016**, *2016* (16), 2851−2857.
(47) Kue, C. S.; Ng, S. Y.; Voon, S. H.; Kamkaew, A.; Chung, L. Y.; Kiew, L. V.; Lee, H. B. Recent Strategies to Improve Boron Dipyrromethene (BODIPY) for Photodynamic Cancer Therapy: An Updated Review. *Photochem. Photobiol. Sci.* **2018**, *17*, 1691−1708.
(48) Wan, Z.; Yu, S.; Wang, Q.; Tobia, J.; Chen, H.; Li, Z.; Liu, X.; Zhang, Y. A BODIPY-Based Far-Red-Absorbing Fluorescent Probe for Hypochlorous Acid Imaging. *ChemPhotoChem* **2022**, *6* (4), No. e202100250.
(49) Peterson, J. A.; Wijesooriya, C.; Gehrmann, E. J.; Mahoney, K. M.; Goswami, P. P.; Albright, T. R.; Syed, A.; Dutton, A. S.; Smith, E. A.; Winter, A. H. Family of BODIPY photocages Cleaved by Single Photons of Visible/Near-Infrared Light. *J. Am. Chem. Soc.* **2018**, *140* (23), 7343−7346.
(50) Weinstain, R.; Slanina, T.; Kand, D.; Klán, P. Visible-to-NIR-Light Activated Release: From Small Molecules to Nanomaterials. *Chem. Rev.* **2020**, *120* (24), 13135−13272.
(51) Sánchez-Carnerero, E. M.; Russo, M.; Jakob, A.; Muchová, L.; Vítek, L.; Klán, P. Effects of Substituents on Photophysical and CO-Photoreleasing Properties of 2,6-Substituted meso-Carboxy BODIPY Derivatives. *Chemistry* **2021**, *3* (1), 238−255.
(52) Lv, W.; Li, Y.; Li, F.; Lan, X.; Zhang, Y.; Du, L.; Zhao, Q.; Phillips, D. L.; Wang, W. Upconversion-Like Photolysis of BODIPY-Based Prodrugs via a One-Photon Process. *J. Am. Chem. Soc.* **2019**, *141* (44), 17482−17486.
(53) Slanina, T.; Shrestha, P.; Palao, E.; Kand, D.; Peterson, J. A.; Dutton, A. S.; Rubinstein, N.; Weinstain, R.; Winter, A. H.; Klán, P. In Search of the Perfect photocage: Structure−Reactivity Relationships in meso-Methyl BODIPY Photoremovable Protecting Groups. *J. Am. Chem. Soc.* **2017**, *139* (42), 15168−15175.
(54) Stafford, A.; Ahn, D.; Raulerson, E. K.; Chung, K.-Y.; Sun, K.; Cadena, D. M.; Forrister, E. M.; Yost, S. R.; Roberts, S. T.; Page, Z. A. Catalyst Halogenation Enables Rapid and Efficient Polymerizations with Visible to Far-Red Light. *J. Am. Chem. Soc.* **2020**, *142* (34), 14733−14742.
(55) Sambath, K.; Zhao, T.; Wan, Z.; Zhang, Y. Photo-Uncaging of BODIPY Oxime Ester for Histone Deacetylases Induced Apoptosis in Tumor Cells. *Chem. Commun.* **2019**, *55* (94), 14162−14165.
(56) Goswami, P. P.; Syed, A.; Beck, C. L.; Albright, T. R.; Mahoney, K. M.; Unash, R.; Smith, E. A.; Winter, A. H. BODIPY-Derived Photoremovable Protecting Groups Unmasked with Green Light. *J. Am. Chem. Soc.* **2015**, *137* (11), 3783−3786.
(57) Soovali, L.; Rodima, T.; Kaljurand, I.; Kütt, A.; Koppel, I. A.; Leito, I. Basicity of some P_1 Phosphazenes in Water and in Aqueous Surfactant Solution. *Org. Biomol. Chem.* **2006**, *4* (11), 2100−2105.
(58) Truong, V. X.; Bachmann, J.; Unterreiner, A.; Blinco, J. P.; Barner-Kowollik, C. Wavelength-Orthogonal Stiffening of Hydrogel Networks with Visible Light. *Angew. Chem., Int. Ed.* **2022**, *61* (15), No. e202113076.

https://doi.org/10.1021/acsami.3c09326
ACS Appl. Mater. Interfaces 2023, 15, 45281−45289